JOURNAL OF MATERIALS SCIENCE **37** (2002) 1497–1502

The influence of Si and Mg rich phases on the mechanical properties of 6061 Al-matrix composites reinforced with Al_2O_3

J. M. GÓMEZ DE SALAZAR, M. I. BARRENA
Departamento de Ciencia de los Materiales e Ingeniería Metalúrgica, Facultad de Ciencias Químicas, Universidad Complutense de Madrid, 28040 Madrid, Spain
E-mail: gsalazar@eucmax.sim.ucm.es
E-mail: ibarrena@eucmax.sim.ucm.es

Besides altering the kinetics of precipitation, the reinforcements with alumina particles appear to alter the relative proportions of the various phases formed in the matrix alloy during ageing. Alumina also seems to reduce the volume fractions of hardening phase in these materials, especially at higher contents. One reason for this effect could be the dislocation relief of the matrix strain associated with the early precipitates. Additionally, the diffusion of Mg and its subsequent incorporation into the reinforcement at the Al_2O_3/Al interface could also result in Mg depletion from the matrix, accounting for the reduction of the β (Mg_2Si) particle sizes. Magnesium incorporation into interfacial alumina to form $MgAl_2O_4$ has been observed in these materials. This paper shows that the nature and morphology of the second phases depend the heat treatment conditions on.

1. Introduction

Al-Mg-Si alloys reinforced with alumina particles are being employed in automotive and aerospace applications [1]. The role of reinforcements in the ageing behaviour of metal-matrix composites (MMCs) has a considerable scientific and technical importance [2]. In general, precipitation of both metastable and equilibrium phases are observed to be accelerated in MMCs. Both nucleation and growth of precipitates can be attributed to the increase of the density of dislocations created from the thermal mismatch between the matrix and the reinforcements which provide additional sites for precipitation and enhance pipe diffusion of solute atoms [3–8].

In these composites the mechanical properties are further compromised by the thermodynamic instability of the phase mixtures and the interfacial reactions [9–11]. The presence of the reinforcement can also considerably influence the response of the matrix alloy under a solubilizated state or under a hardening state [12–14].

The aluminium matrix contains a wide range of second phase particles depending on their chemical composition and the nature of alloying elements [15–17]. The clusters of these particles become heterogeneously distributed during subsequent thermal processing. During solubilization treatments most of the soluble particles from the major alloying additions such as Mg and Si are dissolved. Dispersoids of the Al-Mg-Si-Cu type or the precipitation of Mn, Cr or Zr phases can be formed during annealing treatments [18]. The size and distribution of these various phases depend on time and temperature of the solubilization and/or annealing processes. The distribution and size of particles have a significant influence on the microstructure and mechanical properties of these materials [19, 20].

Therefore the formation of particles removes solute from the matrix and, consequently, changes the strength properties of the matrix material [21, 22]. This fact is especially relevant in alloys treated thermally, where depletion in Mg and Si can significantly change the metastable precipitation processes and age hardening of these materials [23].

2. Experimental procedure

2.1. Materials

The materials used in this work were composites based on an Al-6061 matrix. These matrices contain a 10% (W6A10) or 20% (W6A20) volume fraction of Al_2O_3 particles, which were non-uniform in the shape and have an average diameter of 17 μm for 10% and 23 μm for 20% vol. fraction. Duralcan Co. provided these materials in extruded and a T4 heat treatment condition. The composition of the matrices and of the monolithic alloys were determined using a Jeol 8900 serie M electron probe microanalyser on highly polished surfaces of the specimens and by IPC spectroscopy. The average composition obtained from five different readings for all materials are listed in Table I.

2.2. Methods

The as-received materials were treated by solubilization heat treatment prior to microhardness testing and

TABLE I Chemical compositions of the materials (wt%)

	Element (wt%)								
Material	Si	Fe	Cu	Mn	Mg	Cr	Zn	Ti	Al
AA6061	0.48	0.70	0.20	0.150	1.20	0.11	0.25	0.15	bal
W6A10	0.53	0.08	0.27	0.005	0.89	0.11	0.01	0.01	bal
W6A20	0.55	0.06	0.27	0.004	1.19	0.12	0.01	0.01	bal

differential scanning calorimeter studies (DSC). All samples were heat treated at 560°C ± 0.5°C for 3 hours and quenched in iced water. They were then stored at −20°C before further experiments were performed. In order to investigate the age-hardening behavior of these alloys, samples of all materials were heat treated at 175°C ± 0.5°C for a range of time up to 30 hours. Vicker's testing was performed on an Akashi MVK-A3 microhardness using a 100 g indentation load. All tests were carried out on polished surfaces, without etching. The microhardness values were taken on the matrices from three different samples for each heat treatment condition.

In order to determinate the influence of the temperature on the precipitated phases, subsequent heat treatment were applied to all materials: T6 (solubilized at 560°C ± 0.5°C for 3 hours and quenched in iced water and ageing at 175°C ± 0.5°C during 8 hours and cooling in air) and annealed (solubilized at 560°C ± 0.5°C for 3 hours and cooled in the furnace).

DSC experiments were performed on a Metzler (TA4000) machine. The samples used were discs, 0.6 mm thick and 3 mm diameter, which were obtained by cutting from bulk material in an ultrasonic Gatan 601 machine (26 KHz frequency and using SiC as abrasive). The discs were solution heat treated prior to testing, as described above. All tests were started at 25°C and finished at 500°C, using a heating rate of 10°C/min on three different samples for each type of material studied.

Scanning electron microscopy (SEM-EDS) studies were performed on the samples using a Jeol 6400 (SEM) and a Link EDX microanalyser. All samples were metallographically prepared on polished surfaces using the Keller's reagent to develop the microstructure of samples.

Transmission electron microscopy (TEM) studies were performed to correlate the microstructural changes in MMCs materials with the mechanical properties. Thin slices 50 μm thick were obtained by diamond disc cutting, grinding and finally polishing with a diamond suspension of 1/10 μm in diameter, using ethylenglycol as lubricant. Specimens of 3 mm diameter were ultrasonically cut. The discs were concave polished in a Dimple Grinder Gatan model 656. Finally, an Ion Milling machine, Gatan model 600 (5 Kv, 1 mA, −10°C and an angle of 15°) was used. Microstructural studies and phase identification were carried out by transmission electron microscopy (TEM) using a Jeol 2000 EX operating at 200 KV equipped with a Link (AN1000) X-ray spectrometer.

Mechanical tests (tensile test) were performed for all samples to determine the relationship between the properties and the microestructural changes. Finally, fractographic studies were carried out in order to determine the fracture mechanisms.

3. Results and discussion

3.1. DSC, microhardness and microestructural evaluations

Results from microhardness measurements as a function of aging time at 175°C for the AA6061 alloy and for two composites (W6A10 and W6A20) are shown in Fig. 1. Comparing the three curves (Fig. 1), differences in the behavior of the parent alloy (AA6061) and the matrix composites can be observed.

The parent alloy (AA6061) shows higher hardness than the W6A10 and W6A20, likely. This fact is due to the different precipitation processes that occur in these materials. In DSC curves, (Fig. 2), it can be observed, that the aging process in the MMCs is less pronounced than in the parent materials (AA6061), as a consequence of the lower content of free Mg in the aluminum matrix of the composites. Magnesium and alumina react during the heat treatments giving rise to the formation of the $MgAl_2O_4$ spinel. These reactions can provoke that the precipitation path:

$$GP \rightarrow \beta'' \rightarrow \beta' \rightarrow \beta(Mg_2Si)$$

in the matrix composites with a 10 and 20% volume fraction in Al_2O_3 are inhibited due to the Mg consume

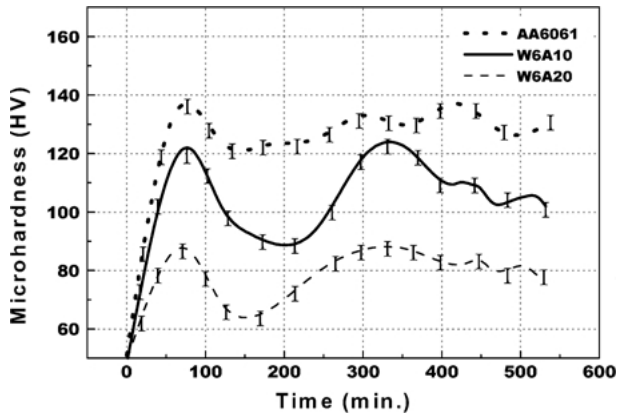

Figure 1 Microhardness profiles as a function of ageing time at 175°C for the AA6061 matrix alloy and for two composites (W6A10 and W6A20).

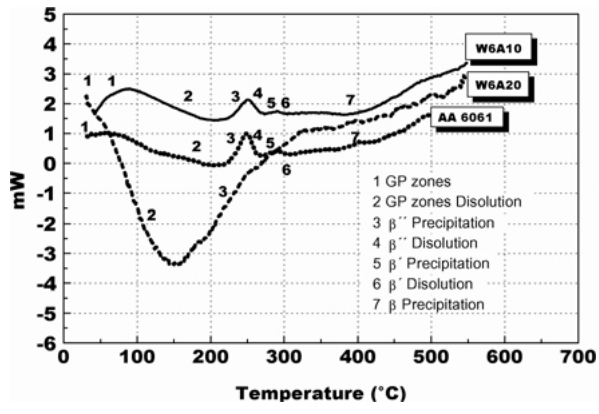

Figure 2 DSC thermograms for the AA6061 matrix alloy and for two composites (W6A10 and W6A20). Error = ±0.5% mW.

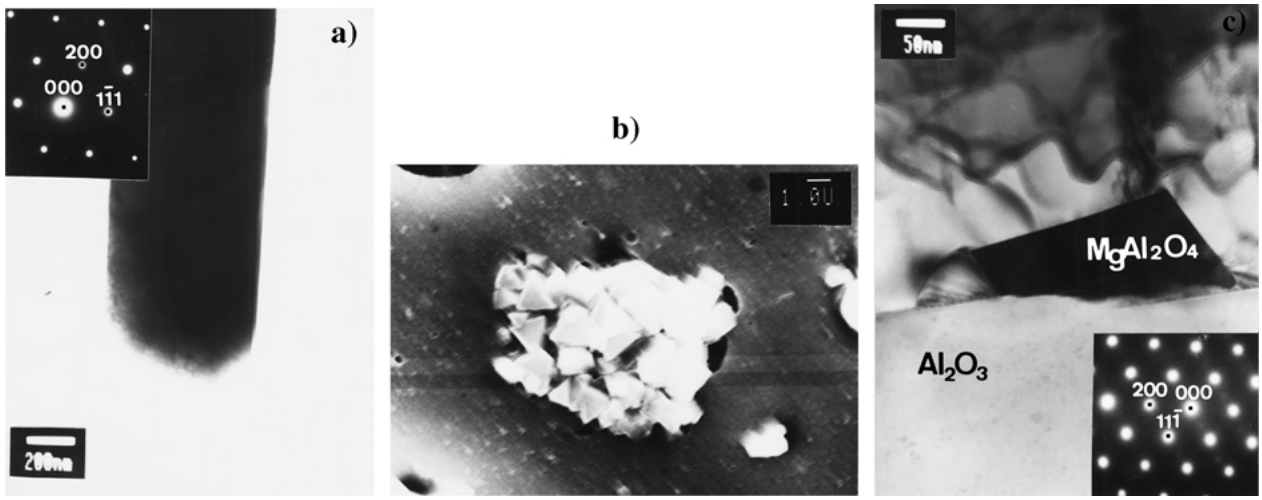

Figure 3 (a) TEM image of β-Mg_2Si phase in the matrix composites with heat treatment T6; [01$\bar{1}$] ED patterns. (b) SEM image of $MgAl_2O_4$ spinel. and (c) TEM image of $MgAl_2O_4$ spinel; [0$\bar{1}$1] ED patterns.

in the matrix, as deduced by comparing the DSC and the microhardness curves for the composites.

The equilibrium β-Mg_2Si phase in plate form (Fig. 3a) was observed in all materials with heat treatment T6 and in minor percentage in matrix composites than in the parent alloy. It presents a cubic symmetry with a cell parameter $a = 6.3675$ Å.

On the other hand, images obtained by SEM (Fig. 3b) and TEM (Fig. 3c) in both composites and heat conditions, show $MgAl_2O_4$ spinel growing in aluminum matrix and on the Al_2O_3 crystals. Spinel has a cubic structure with lattice parameter of $a = 8.0813$ Å, and was found in higher percentage in annealing heat condition.

Additionally to β-Mg_2Si phase and $MgAl_2O_4$ spinel in the matrix composites with heat treatment T6, two second phases were identified in the matrix alloy with any element (Si), which are necessary to form the hardness precipitates: Al_3FeSi and amorphous Si_XO_Y.

3.1.1. Al_3FeSi phase

The typical morphology of these phases is shown in Fig. 4. The particles had sheet form of 4 μm size. The chemical information was obtained by EDS, showing a monoclinic symmetry, with cell parameters $a = 18.8033$ Å, $b = 10.015$ Å, $c = 9.2345$ Å and $\beta = 133.631°$. In this way, these particles were identified as the γ-Al_3FeSi phase.

3.1.2. Amorphous Si_XO_Y

Another type of particle frequently found in this alloy contained a very high concentration of Si (Fig. 5a) with a size of 600 nm and idiomorphic shape. X-ray diffraction analysis showed no evidence of crystallinity. They always appeared dark in the bright-field images (Fig. 5b) and showed no change in contrast with specimen tilt. With these data, these particles were identified as the amorphous Si_XO_Y phase.

In the case of composites with annealing heat treatment the ternary and quaternary phases appear due to the temperature and cooling rate conditions improve the diffusion processes. Additionally to the kept phases,

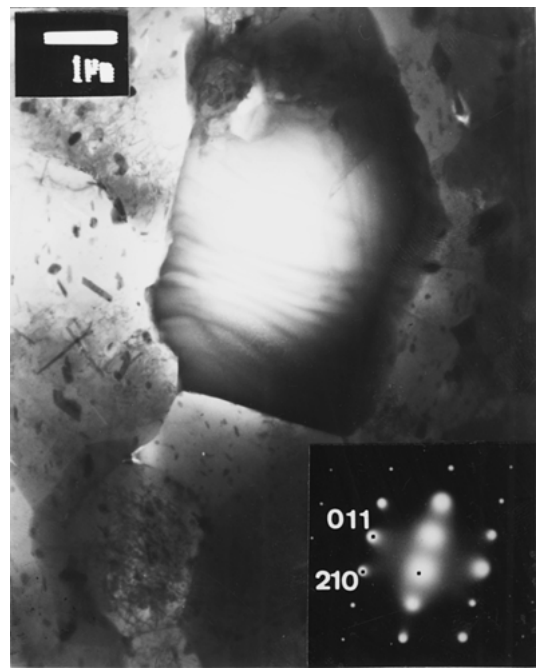

Figure 4 TEM image of Al_3FeSi phase with a [122] ED pattern.

other three ones were identified in the AA6061 matrix annealed: Al_2CuMg, Mg_2SiO_4 and $Al_{1.9}CuMg_{4.1}Si_{3.3}$, in small amount, which are descripted below.

3.1.3. Al_2CuMg phase

A phase with plate form and 3 μm of size was found in boundary grain. A [100] ED pattern of a particle (Fig. 6) allowed to identify the Al_2CuMg phase which has orthorhombic symmetry, with lattice parameters $a = 4.0086$ Å, $b = 9.2437$ Å and $c = 7.1455$ Å. This phase form at 460°C during slow cooling, therefore the appearance of this phase is favoured in the heat treatment applied.

3.1.4. Mg_2SiO_4 phase

These particles appear to have needles shape with 15 μm of length. Some examples are shown in Fig. 7. Measurements of lattice spacing from [001] electron diffraction pattern have shown that the lattice

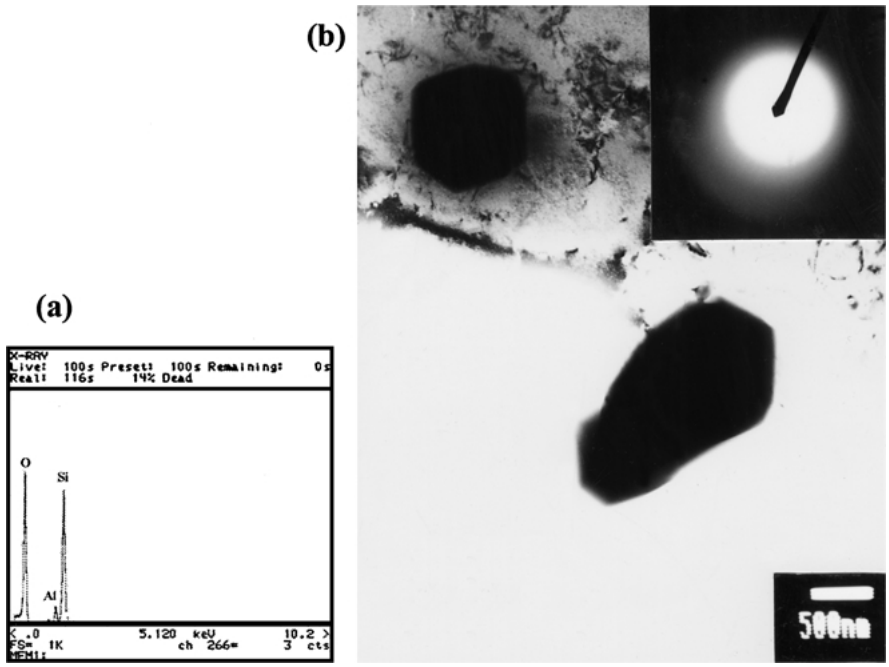

Figure 5 (a) EDX analysis of the precipitates; (b) Electron diffraction analysis and TEM image of amorphous Si_XO_Y phase.

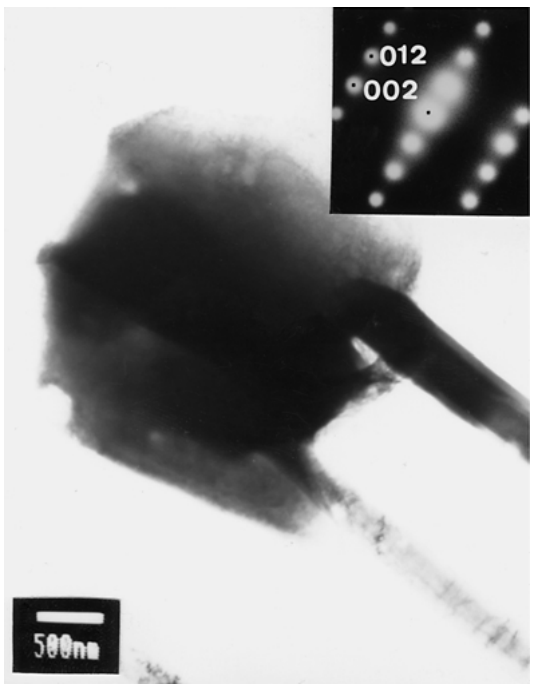

Figure 6 TEM image of Al_2CuMg phase with a [100] ED pattern of Al_2CuMg phase.

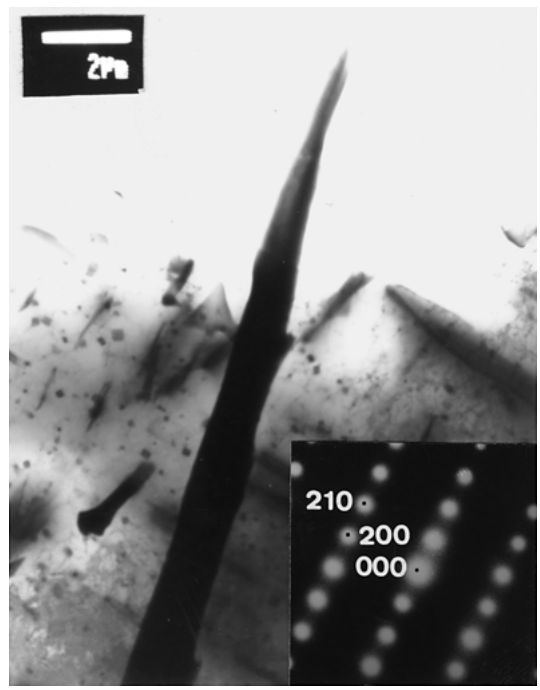

Figure 7 TEM image of Mg_2SiO_4 phase with a [001] ED pattern of Mg_2SiO_4 phase.

parameters of this phase is $a = 8.2243$ Å, however the crystal structure was determined to be cubic.

3.1.5. $Al_{1.9}CuMg_{4.1}Si_{3.3}$ phase

This type of particles was less observed in the matrix as compared with studied phases before. They are usually small, in the range of 50 nm and spherical shape as observed in the micrograph of Fig. 8. The particles were identified to have a hexagonal structure with lattice parameters of $a = 10.3463$ Å and $c = 4.0085$ Å.

3.2. Mechanical properties evolution

From these tests, we can deduce that the intermetallic precipitation obtained with the different heat treatments bring out the most interesting changes in the mechanical properties of the composites.

Table II shows tensile strength and the yield strength of the parent alloy (AA6061) and the W6A10 and W6A20 composites. It can be deduced that both composites present a higher yield strength and tensile strength in relation to the parent alloy. The increases in the tensile strength are 15% (W6A10) and 26% (W6A20), in T6 condition. In relation to the yield strength the increase are 20% (W6A10) and 39% (W6A20). On the other hand the loss of elongation in the composites in relation to the AA6061 in the same heat treated conditions is 60% (W6A10) and 73% (W6A20). In the case of annealed condition, the

TABLE II Tensile values for the AA6061 alloy and composites (W6A10 and W6A20)

Materials	Heat treatment	Tensile strength (MPa)	0.2% Proof stress (MPa)	Elongation (%)
AA6061	T6	330	270	15
AA6061	Annealed	127	76	25
W6A10	T6	375	330	6
W6A10	Annealed	156	95	20
W6A20	T6	408	375	4
W6A20	Annealed	160	96	13

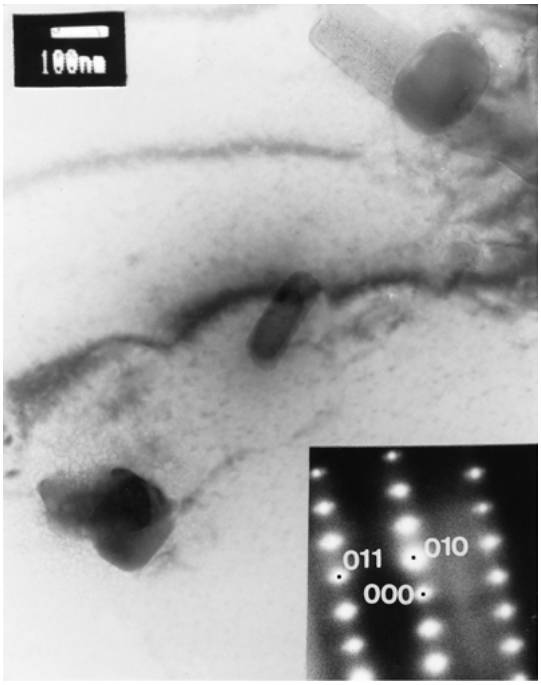

Figure 8 TEM image of $Al_{1.9}CuMg_{4.1}Si_{3.3}$ phase; with a [100] ED pattern of $Al_{1.9}CuMg_{4.1}Si_{3.3}$ phase.

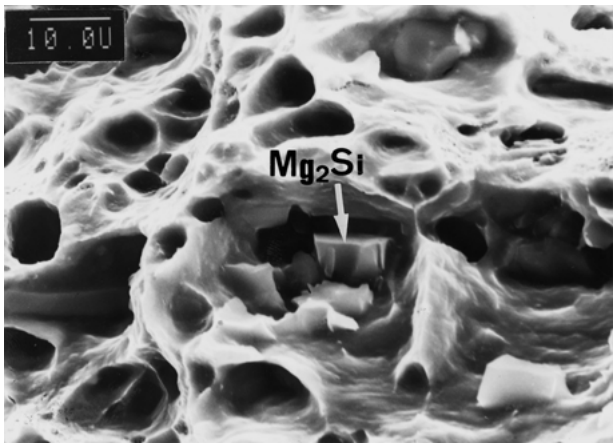

Figure 9 Ductile fracture with Mg_2Si in the matrix composites.

increase both tensile strength and yield strength is approximately of 25% about parent material (AA6061).

Broken surfaces in different thermal conditions and in different mechanical tests were studied by SEM-EDS techniques in order to determine the fracture mechanism in these materials. Fig. 9 shows the broken surfaces of the W6A10 in T6 condition. The fracture type is ductile and intermetallic compounds similar to Mg_2Si appear in the voids. When the Al_2O_3 particles have a

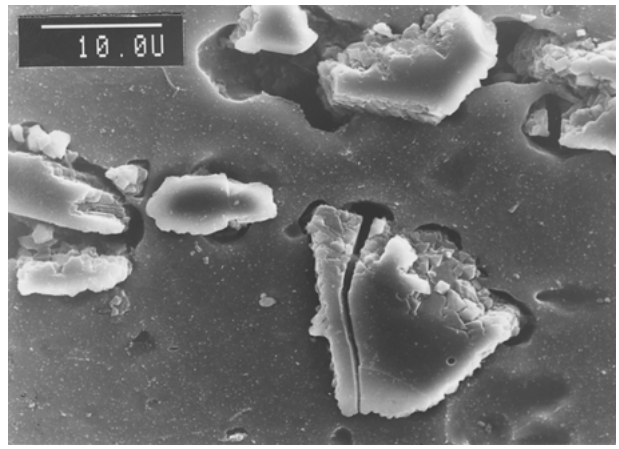

Figure 10 Fracture in Al_2O_3 particle with a size larger than 15 μm.

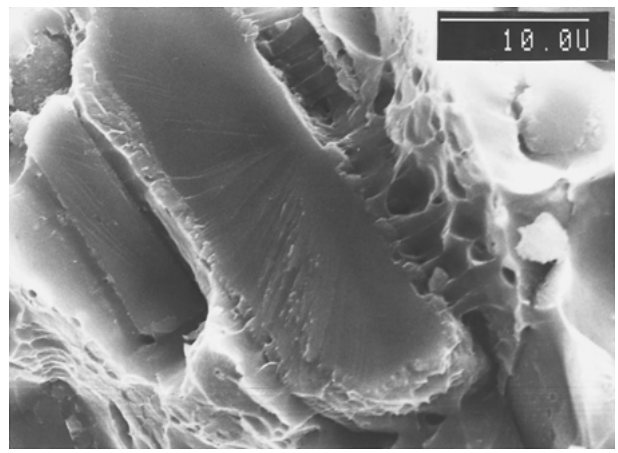

Figure 11 Cracks grow into the alumina particles when the interfacial reaction takes place.

size more than 15 μm these can appear fractured, as shown in Fig. 10. However, when the interfacial reaction takes place between the matrix and Al_2O_3 particles ($MgAl_2O_4$), then cracks grow into the alumina particles (Fig. 11).

These facts indicate that the percentage of reinforced particles is the principal response of the mechanical properties changes, in the same heat treatment condition. T6 heat treatment combines the maximum values both volume fractions of reinforced particles and hardening phase (Mg_2Si). Secondary phases precipitated in the composite matrix do not modify directly mechanical property values of these materials. However these phases remove any element as Si and Mg, which are necessary to form the hardening precipitates.

4. Conclusions

1. This investigation shows that the nature and morphology of second and ternary silicium and/or magnesium rich phases in composites matrix, are depend upon the heat treatment condition. The temperature and cooling rate conditions improve the diffusion process.

2. The parent alloy (AA6061) shows higher microhardness than the matrix W6A10 and W6A20 composites. This fact is due to the lower content of free Mg and Si, necessary to form hardening phase, in the aluminum matrix of the composites.

3. The precipitation sequence of β-Mg_2Si phase in AA6061 is unaffected by the addition of alumina particles. However, the formation of the $MgAl_2O_4$ spinel by reaction of Mg and Al_2O_3 and the secondary phases precipitation, inhibit the precipitation processes of the β-Mg_2Si phase.

4. The mechanical properties of composites increase when the volume fraction of reinforced is higher. The secondary phases precipitation in the composites matrix, remove elements which are necessary to form matrix hardening phase.

Acknowledgements

The authors wish to thank CAM for the financial support of this work under the 07N/0038/98 project.

References

1. A. M. SAMUEL and F. H. SAMUEL, *Key Eng. Mater.* **104–107** (1995) 65.
2. N. R. M. R. BHARGAVA, I. SAMAJDAR, S. RANGANATHAN and M. K. SURAPPA, *Metall. Mater. Trans.* A **29A** (1998) 2835.
3. I. DUTTA, S. M. ALLEN and J. L. HAFLEY, *ibid.* **22A** (1995) 1553.
4. G. BIROLI, G. CAGLIOTI, L. MARTINI and G. RIONTINO, *Scripta Metall. Mater.* **39**(2) (1998) 197.
5. P. APPENDINO and C. BADINI, *Mater. Sci. Eng.* **A135** (1991) 275.
6. T. DAS, S. BANDYOPADHYAY and S. J. BLAIRS, *J. Mater. Sci.* **29** (1994) 5680.
7. *Idem.*, in Proc. Conf. ICCM/9 Metal Matrix Composites Madrid (1995) Vol. I, p. 424.
8. P. MERLE, D. DAFIR and S. M. SEYED REYHANI, in Proc. Conf. ICCM/9 Metal Matrix Composites Madrid (1995) Vol. I, p. 401.
9. S. IKENO, M. ARAKI, K. MATSUDA, F. SHINAGAWA and Y. UETANI, *J. Japan Inst. Light Met.* **49**(6) (1999) 244.
10. D. YU and T. CHANDRA, *Mater. Trans., JIM* **34**(12) (1993) 1184.
11. J. WANG, M. FURUKAWA, Z. HORITA, M. NEMOTO, Y. MA and T. G. LANGDON, *Metall. Mater. Trans.* A **26A** (1995) 581.
12. D. J. LOYD, I. JIN and G. C. WEATHERLY, *Scripta Metall. Mater.* **31**(4) (1994) 393.
13. A. D. MCLEOD and C. M. GABRYEL, *Metall. Mater. Trans.* A **23A** (1992) 1279.
14. J. C. LEE, G. H. KIM and H. I. LEE, *Mater. Sci. Technol.* **13** (1997) 182.
15. J. K. PARK and A. J. ARDELL, *Acta Metall.* **34**(12) (1986) 2399.
16. P.A. THACKERY, *J. Inst. Metals* **96** (1968) 228.
17. S. K. TANG and T. SRITHARAN, *Mater. Sci. Technol.* **14** (1998) 738.
18. A. K. GUPTA, P. H. MAROIS and D. J. LLOYD, *Mater. Char.* **37** (1996) 61.
19. M. GAO, C. R. FENG and R. P. WEI, *Metall. Mater. Trans.* A **29A** (1998) 1145.
20. A. K. GUPTA and D. J. LLOYD, *ibid.* **30A** (1999) 879.
21. S. IKENO, K. MATSUDA and S. RENGAKUJI, *J. Mater. Sci.* **36** (2001) 1921.
22. M. TAN, Q. XIN, Z. LI and Y. ZONG, *ibid.* **36** (2001) 2045.
23. D. SUN, X. C. SUN, D. O. NORTHWOOD and J. H. SOKOLOWSKY, *Mater. Char.* **36** (1996) 83.

Received 29 June
and accepted 4 December 2001